

UNCLASSIFIED **CONFIDENTIAL**

C.2  
Copy 6  
RM L55E17a



# RESEARCH MEMORANDUM

LOADS ON WINGS DUE TO SPOILERS AT SUBSONIC  
AND TRANSONIC SPEEDS

By Alexander D. Hammond

Langley Aeronautical Laboratory

Langley Field, Va.

UNCLASSIFIED

Authority of

*NASA TPA 9*

Date

*9-1-59*

*NB 11-20-59*

CLASSIFIED DOCUMENT

This material contains information affecting the National Defense of the United States within the meaning of the espionage laws, Title 18, U.S.C., Secs. 793 and 794, the transmission or revelation of which in any manner to an unauthorized person is prohibited by law.

**NATIONAL ADVISORY COMMITTEE  
FOR AERONAUTICS**

**WASHINGTON**

June 27, 1955

**CONFIDENTIAL**



## NATIONAL ADVISORY COMMITTEE FOR AERONAUTICS

## RESEARCH MEMORANDUM

LOADS ON WINGS DUE TO SPOILERS AT SUBSONIC  
AND TRANSONIC SPEEDS

By Alexander D. Hammond

## SUMMARY


Some of the results of several of the more recent investigations made in the Langley 7- by 10-foot tunnels are presented to illustrate the magnitude and distribution of the additional loads on wings resulting from projection of spoiler-type controls. The results show that, although there is no known pure theoretical method for determining the magnitude or the point of application of the additional load due to spoiler projection on a given wing, wind-tunnel test data on wings close to the desired configuration can be used to estimate with a fair degree of accuracy the additional loads associated with spoiler-type controls.

## INTRODUCTION

The spoiler is being used more and more on present-day aircraft for lateral control. In order to illustrate the variation of the magnitude and distribution of the additional loads on wings resulting from spoiler projection with changes in angle of attack, speed, and geometry of the wing and spoiler, some of the results of several of the more recent investigations made in the Langley 7- by 10-foot tunnels will be presented.

## COEFFICIENTS AND SYMBOLS

$c_n$	section normal-force coefficient, $\frac{\text{Normal force}}{qc}$
$C_N$	wing normal-force coefficient, $\frac{\text{Wing normal force}}{qS}$
$C_B$	wing bending-moment coefficient, $\frac{\text{Wing bending moment}}{q \frac{S}{2} \frac{b}{2}}$



$P_R$	resultant pressure coefficient, $\left(\frac{p - p_o}{q}\right)_u - \left(\frac{p - p_o}{q}\right)_l$
$A$	aspect ratio, $b^2/S$
$b$	wing span, ft
$c$	local wing chord measured in planes parallel to wing plane of symmetry, ft
$c_{av}$	average wing chord, $\frac{c_r + c_t}{2}$ , ft
$c_f$	flap chord, ft
$M$	Mach number
$p$	static pressure, lb/sq ft
$p_o$	free-stream static pressure, lb/sq ft
$q$	free-stream dynamic pressure, $\frac{1}{2}\rho V^2$ , lb/sq ft
$S$	wing area, sq ft
$t$	wing maximum thickness, ft
$V$	free-stream air velocity, ft/sec
$x$	chordwise distance from wing leading edge, ft
$\Delta x_{cp}$	chordwise distance of center of pressure resulting from control deflection from wing leading edge, ft
$y$	spanwise distance from plane of symmetry, ft
$\Delta$	increment resulting from control deflection
$\alpha$	angle of attack of wing, deg
$\delta$	control deflection
$\Lambda$	sweep angle, deg
$\lambda$	taper ratio; ratio of tip chord to root chord, $c_t/c_r$

$\rho$  mass density of air, slugs/cu ft

Subscripts:

cp center of pressure

d deflector

f flap

u upper wing surface

l lower wing surface

### DISCUSSION

In figure 1 are shown the model configurations and test conditions for the investigations made in the Langley 7- by 10-foot tunnels. A pressure-distribution investigation utilizing a  $30^\circ$  sweptback-wing-fuselage model (model A) having an aspect ratio of 3, a taper ratio of 0.5, and NACA 65A004 airfoil section parallel to the plane of symmetry was made at a Mach number of 0.26 for an angle-of-attack range from  $-4^\circ$  to  $24^\circ$ . The right wing of the model was equipped with two of the more common types of spoiler controls, a plain spoiler and a spoiler slot deflector. These controls were tested for a range of spoiler projection from 0 to 12 percent of the local chord and a range of deflector projection from 0 to 9 percent of the local chord. The results of this investigation are unpublished.

Force tests were made on model B, an unswept semispan wing having an aspect ratio of 4, a taper ratio of 0.6, and NACA 65A006 airfoil sections parallel to the plane of symmetry, through a Mach number range from 0.62 to 1.20 for angles of attack from  $-4^\circ$  to  $20^\circ$ . Model B was equipped with a plain spoiler and a spoiler slot deflector, extending from the 40- to the 97-percent-semispan stations; tests were made for spoiler projections from 0 to 10 percent of the local chord and for deflector projections from 0 to 7.5 percent of the local chord. The results of this investigation are published in reference 1.

Force tests were also made on a series of unswept untapered semispan wings, represented by model C, having aspect ratios from 1 to 6 and two airfoil sections, NACA 65A004 and NACA 65A006, parallel to plane of symmetry. A plain flap-type spoiler projected to a height of 7.5 percent chord was tested along the 40-, 60-, 80-, and 100-percent-chord lines of the wings through a Mach number range from 0.6 to 1.1 at angles of attack from  $-10^\circ$  to  $25^\circ$ . These tests are also unpublished.

The results of the pressure-distribution measurements taken at the six spanwise stations on the right wing of model A are used to show, in figure 2, the variation of the wing-section normal-force coefficient  $c_n$  with spanwise position  $y/b/2$  from the wing-fuselage junction to the wing tip for the plain wing at angles of attack of  $2^\circ$  and  $8^\circ$ . The spoiler was projected to 12 percent of the local chord and the deflector was projected to 9 percent of the local chord. At both angles of attack ( $2^\circ$  and  $8^\circ$ ), projection of the spoiler slot deflector considerably decreased the loading over that portion of the wing span covered by the control.

Inasmuch as the incremental loads due to spoiler projection, that is, the differences between the plain-wing curves and the curves for the spoiler slot deflector, are of primary interest, the incremental loadings obtained from plots similar to figure 2 have been normalized and replotted in figure 3 to show the variation of the incremental section normal-force coefficient per unit incremental wing normal-force coefficient  $\frac{\Delta c_n}{\Delta c_{n_{av}}}$  with spanwise location from the wing-fuselage junction to the wing tip. The theoretical curve was obtained by the method of DeYoung outlined in references 2 and 3 for flap-type controls having the same span as the spoilers of model A on a wing having the same geometric characteristics as the wing of model A. Since the spoilers are deflected only on the right wing of model A, the theoretical curve is the average between the curve obtained for symmetrically deflected flaps and unsymmetrically deflected flaps from references 2 and 3, respectively. The experimental points denoted by the circled symbols were for an angle-of-attack range from  $-4^\circ$  to  $6^\circ$ .

At the top of figure 3 are curves of the variations of the incremental wing normal-force coefficient  $\Delta C_N$  and incremental wing bending-moment coefficient  $\Delta C_B$  with angle of attack for the spoiler slot deflector projected to heights of 12 and 9 percent of the local chord. In the angle-of-attack range from  $-4^\circ$  to  $6^\circ$ , there is an increase in both the incremental normal force and bending moments with increase in angle of attack although there is little change of the distribution of this load with change in angle of attack and the experimental and theoretical span load distributions are in good agreement (fig. 3). At angles of attack above about  $6^\circ$ , there is separation in the flow over the wing near the wing tip and the inboard end of the spoiler, and the experimental distributions would not be expected to agree with theory.

The chordwise load distribution resulting from spoiler projection will now be considered. The results of the pressure-distribution measurements made at the midsemispan station of model A have been used to show, in figure 4, the chordwise resultant pressure distribution due to two types of spoiler controls. Figure 4 gives the variation of the

incremental resultant pressure coefficient  $\Delta P_R$  with chordwise location  $x/c$  expressed in terms of the local chord for plain spoilers (denoted by solid curves) and for spoiler slot deflectors (denoted by the dashed curves). These data were for an angle of attack of  $0^\circ$ . The projection chosen for the two types of spoiler controls was such that they gave approximately equal section normal-force coefficients. Because of the load carried on the deflector itself (fig. 4), which is located well back on the wing, the center of pressure for the spoiler slot deflector is behind the center of pressure for the plain spoiler. Figure 5 shows the variation of the center-of-pressure location of the section incremental normal force  $\frac{\Delta x_{cp}}{c}$  with span for a plain spoiler projected to a height of 12 percent chord and for a spoiler slot deflector projected to heights of 12 and 9 percent chord on model A at an angle of attack of  $0^\circ$ . The center of pressure for the spoiler slot deflector lies along approximately the 43-percent-chord line across the wing span and the center of pressure for the plain spoiler is from 10 to 30 percent further forward on the wing.

Although there were no pressure-distribution measurements made on model B to obtain the variation of the center-of-pressure location across the wing span, the results of the force tests on model B have been used to show (fig. 6) the variation of the center-of-pressure location of the incremental wing normal force with angle of attack at Mach numbers of 0.84 and 1.20. The spoiler was deflected to 10 percent chord (see solid curves); the spoiler slot deflector was projected to 10 and 7.5 percent chord (see dashed curves).

The results shown in figure 6 indicate that the center-of-pressure locations of the incremental wing normal force are about 10 percent further forward on the wing for the plain spoiler than the center-of-pressure locations of the spoiler slot deflector at all angles of attack at the Mach numbers shown. There are variations in the centers of additional load with angle of attack; however, the trends of this variation for the two types of spoilers are similar at the Mach numbers shown and at the other Mach numbers investigated. It then follows that the results of force tests on plain spoilers can be used to determine the center-of-pressure location of the incremental normal force resulting from projection of spoiler slot deflectors.

Results of the investigation made on the unswept wings denoted by model C can be used to show the changes in the chordwise position of the center-of-pressure location with such variables as wing thickness, wing aspect ratio, and spoiler chordwise position. The data for the aspect-ratio-6, 6-percent-thick wing have been used to show (fig. 7) the variation of the center-of-pressure location of the incremental section normal force with Mach number at an angle of attack of  $0^\circ$  for spoilers

projected to 7.5 percent chord and located along the 40-, 60-, 80-, and 100-percent-chord lines and, for comparison, data on a 23-percent-chord flap-type control are also presented (dashed curve).

As the spoilers move rearward on the wing, the center-of-pressure location moves toward the wing trailing edge at all Mach numbers tested. Although there is little variation in the center of additional load with Mach number for spoilers located along the 80-percent-chord line, spoilers located along the 100-percent-chord line have centers of pressure that are located near the wing trailing edge at transonic Mach numbers as does the plain flap-type control. In order to show the variation of the center-of-pressure location with Mach number at other angles of attack, the data for the spoilers located along the 80-percent-chord line have been plotted on the right-hand side of figure 7 for angles of attack from  $0^\circ$  to  $10^\circ$ . At all Mach numbers investigated, the center-of-pressure location moves toward the wing trailing edge with increase of angle of attack up to  $10^\circ$ , and limited data indicate that the centers of additional load move back toward the wing leading edge with further increase in angle of attack.

The trends shown for the aspect-ratio-6, 6-percent-thick wing of the variation of the center-of-pressure location with Mach number are similar to the trends found for other wings of this series. The variation of the center-of-pressure location of the incremental wing normal-force coefficient with aspect ratio at an angle of attack of  $0^\circ$  is shown in figure 8 for spoilers located along the 60-, 80-, and 100-percent-chord lines of the 4- and 6-percent-thick wings at a Mach number of 0.80. The dashed curves are for the spoilers on the 4-percent-thick wings and the solid curves are for the spoilers on the 6-percent-thick wings. At all aspect ratios investigated, moving the spoilers rearward on the wing moves the center-of-pressure location toward the wing trailing edge. Although there is little variation of the center-of-pressure location with aspect ratio for spoilers located along the 80-percent-chord line on either the 4- or 6-percent-thick wings, the center-of-pressure locations for spoilers on the 4-percent-thick wings are approximately 8 to 10 percent further forward on the wing than are the center-of-pressure locations for spoilers on the 6-percent-thick wings. In order to show the variation of the center-of-pressure location with aspect ratio at angles of attack other than  $0^\circ$ , the data for spoilers located along the 80-percent-chord line on the 6-percent-thick wings have been plotted on the right-hand side of figure 8 for angles of attack from  $0^\circ$  to  $10^\circ$ . At this Mach number there is very little variation of the center-of-pressure location with aspect ratio at any angle of attack up to  $10^\circ$ , although the center of pressure generally moves forward on the wing with increase in angle of attack for the spoiler on wings having aspect ratios from 1 to 5.

## CONCLUDING REMARKS

It should be pointed out that there is no known pure theoretical method for determining either the magnitude or the point of application of the additional load due to spoiler projection on a given wing. However, if force tests on configurations close to the desired configuration are used to estimate the magnitude of the additional load and its point of application, and if this load is distributed according to the theoretical load distribution of flap-type controls of the same span, the additional root bending moment and wing twisting moment can be determined in the subsonic and transonic speed range at low angles of attack with a fair degree of accuracy.

Langley Aeronautical Laboratory,  
National Advisory Committee for Aeronautics,  
Langley Field, Va., April 26, 1955.

## REFERENCES

1. Vogler, Raymond D.: Wind-Tunnel Investigation at Transonic Speeds of a Spoiler-Slot-Deflector Combination on an Unswept NACA 65A006 Wing. NACA RM L53J21, 1953.
2. DeYoung, John: Theoretical Symmetric Span Loading Due to Flap Deflection for Wings of Arbitrary Plan Form at Subsonic Speeds. NACA Rep. 1071, 1952. (Supersedes NACA TN 2278.)
3. DeYoung, John: Theoretical Antisymmetric Span Loading for Wings of Arbitrary Plan Form at Subsonic Speeds. NACA Rep. 1056, 1951. (Supersedes NACA TN 2140.)



## MODEL CONFIGURATIONS

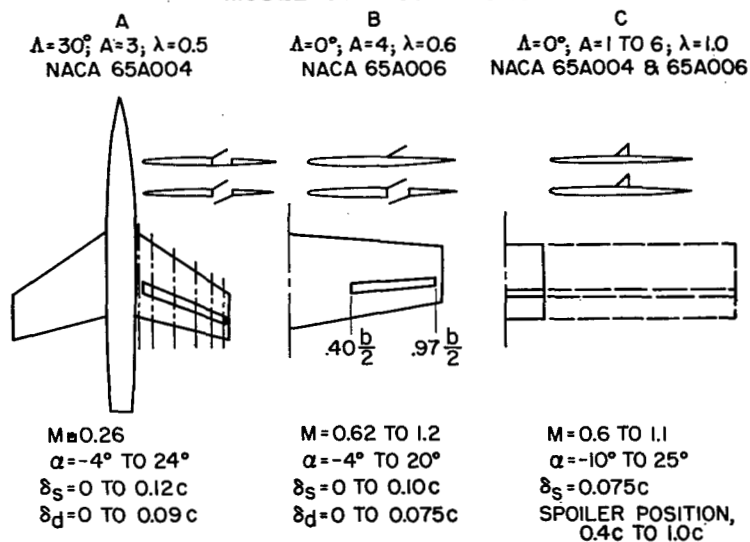


Figure 1

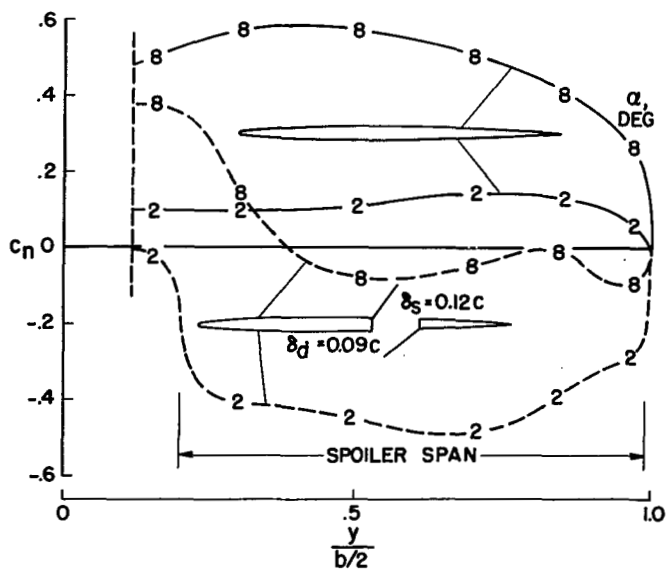
SPANWISE LOAD DISTRIBUTION WITH AND WITHOUT SPOILER  
MODEL A

Figure 2

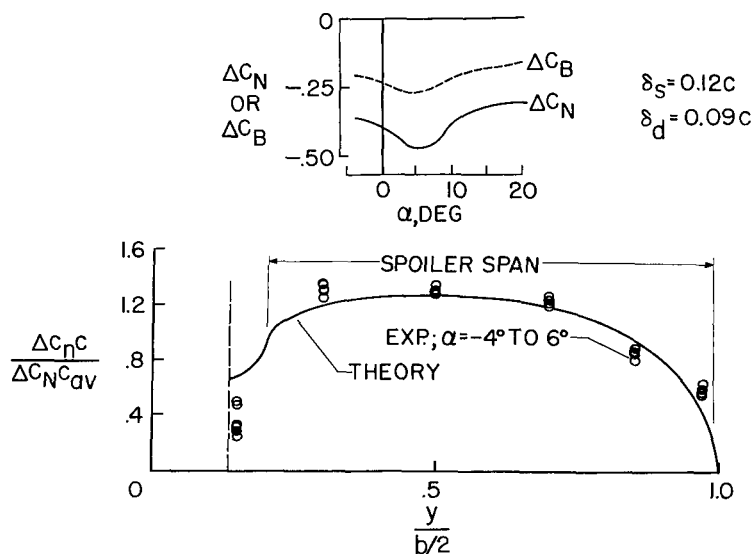
SPANWISE ADDITIONAL LOAD DISTRIBUTION  
MODEL A

Figure 3

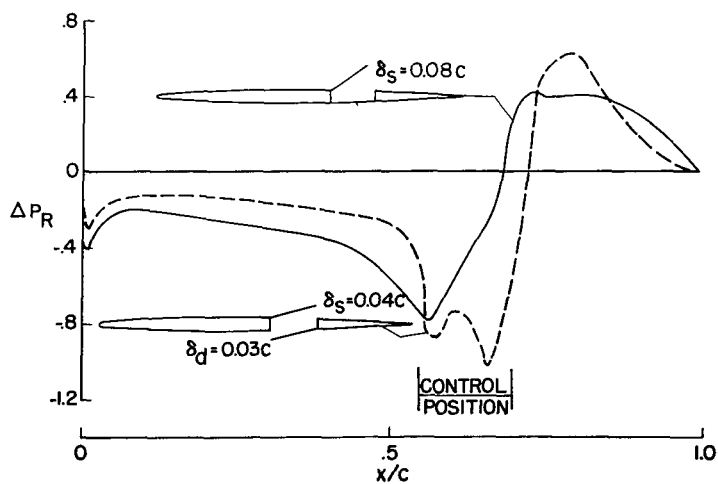
CHORDWISE RESULTANT PRESSURE  
DISTRIBUTION DUE TO SPOILERSMODEL A ;  $\alpha = 0^\circ$ 

Figure 4

VARIATION OF LOCAL CHORDWISE CENTERS OF PRESSURE  
MODEL A;  $\alpha = 0^\circ$

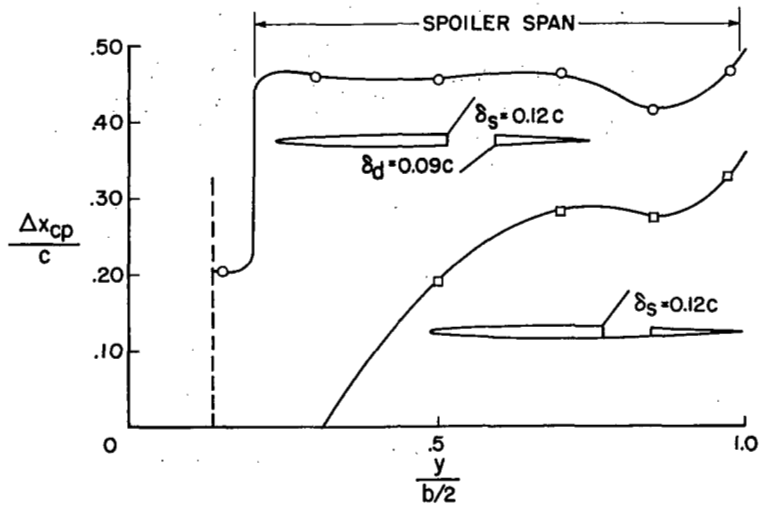


Figure 5

VARIATION OF CHORDWISE CENTERS OF ADDITIONAL LOAD  
WITH ANGLE OF ATTACK

MODEL B

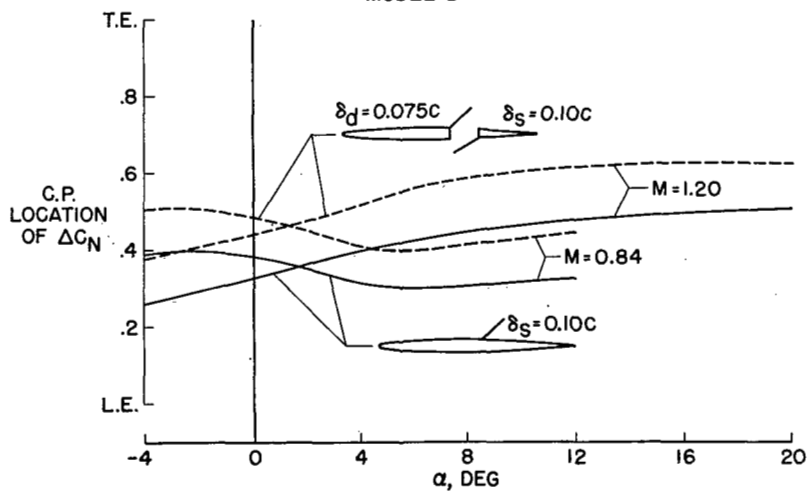


Figure 6

# VARIATION OF CHORDWISE CENTERS OF ADDITIONAL LOAD WITH MACH NUMBER

MODEL C;  $A = 6$ ;  $t/c = 0.06$

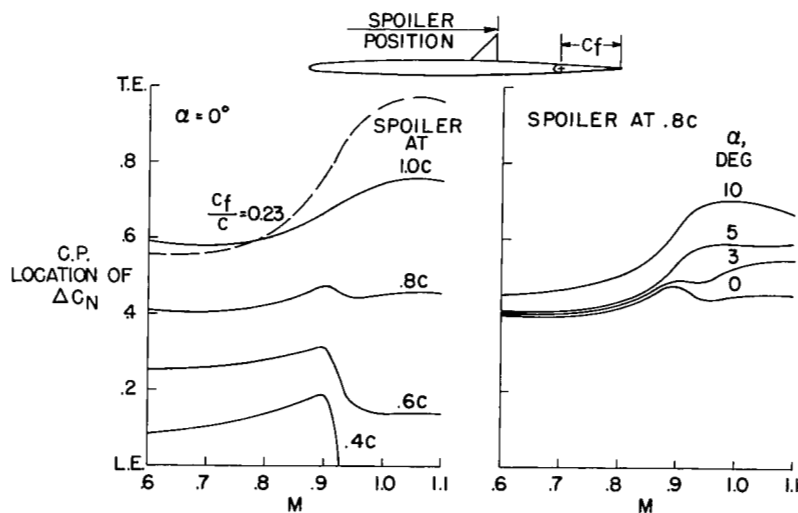


Figure 7

# VARIATION OF CHORDWISE CENTERS OF ADDITIONAL LOAD WITH ASPECT RATIO

MODEL C,  $M = 0.8$

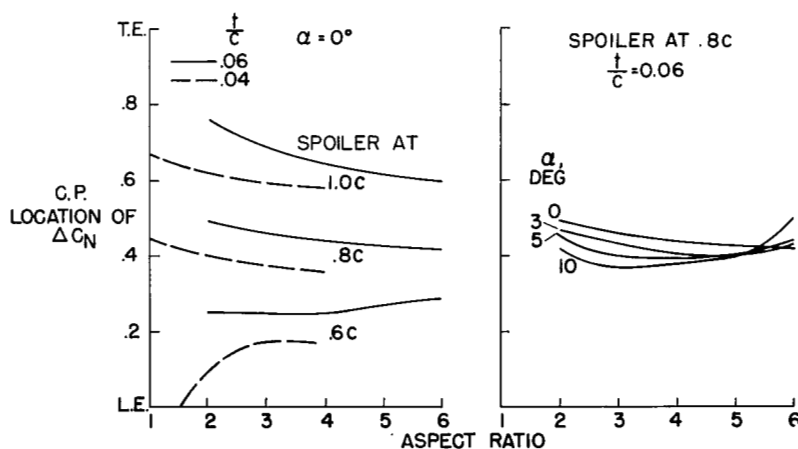


Figure 8

NASA Technical Library



3 1176 01437 6827

**CONFIDENTIAL**